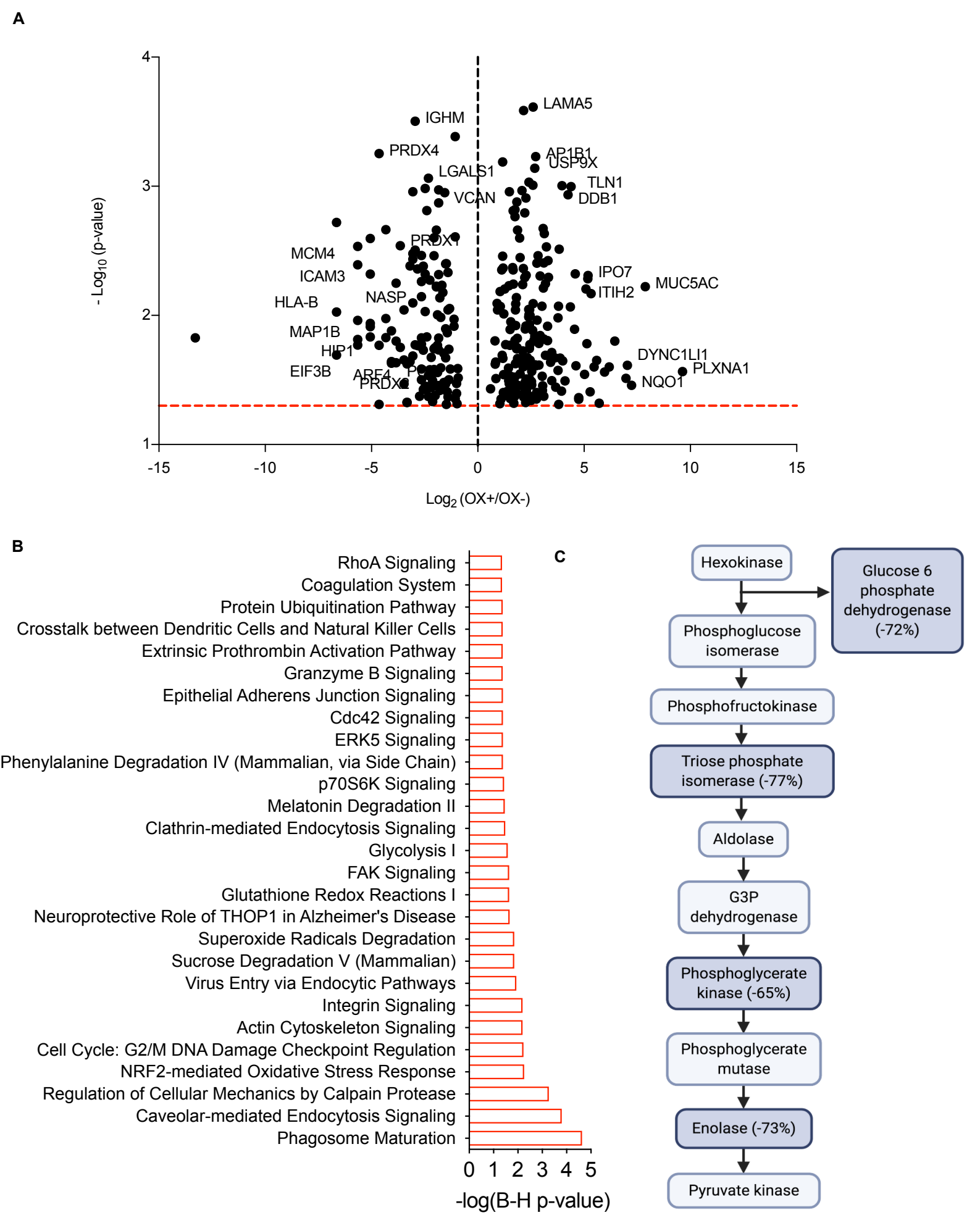

Figure S1: Proteomic comparison of PZ_{OX+} and PZ_{OX-} LUAD tumors. A) Comparative proteomics between PZ_{OX+} and PZ_{OX-} tumors using label free proteomics. The proteins that differed between the two groups are shown in the Volcano plot (Anova; $p<0.05$). **B)** The cellular functions associated with the proteins differentially expressed in PZ_{OX+} versus PZ_{OX-} were analyzed using IPA (Qiagen) and ranked by significance (Fisher's Exact Test with multiple corrections). **C)** Glucose metabolizing proteins downregulated in OX+_LUADs. The reduction is shown as percentage of inhibition (PZ_{OX-} as % of PZ_{OX+}).

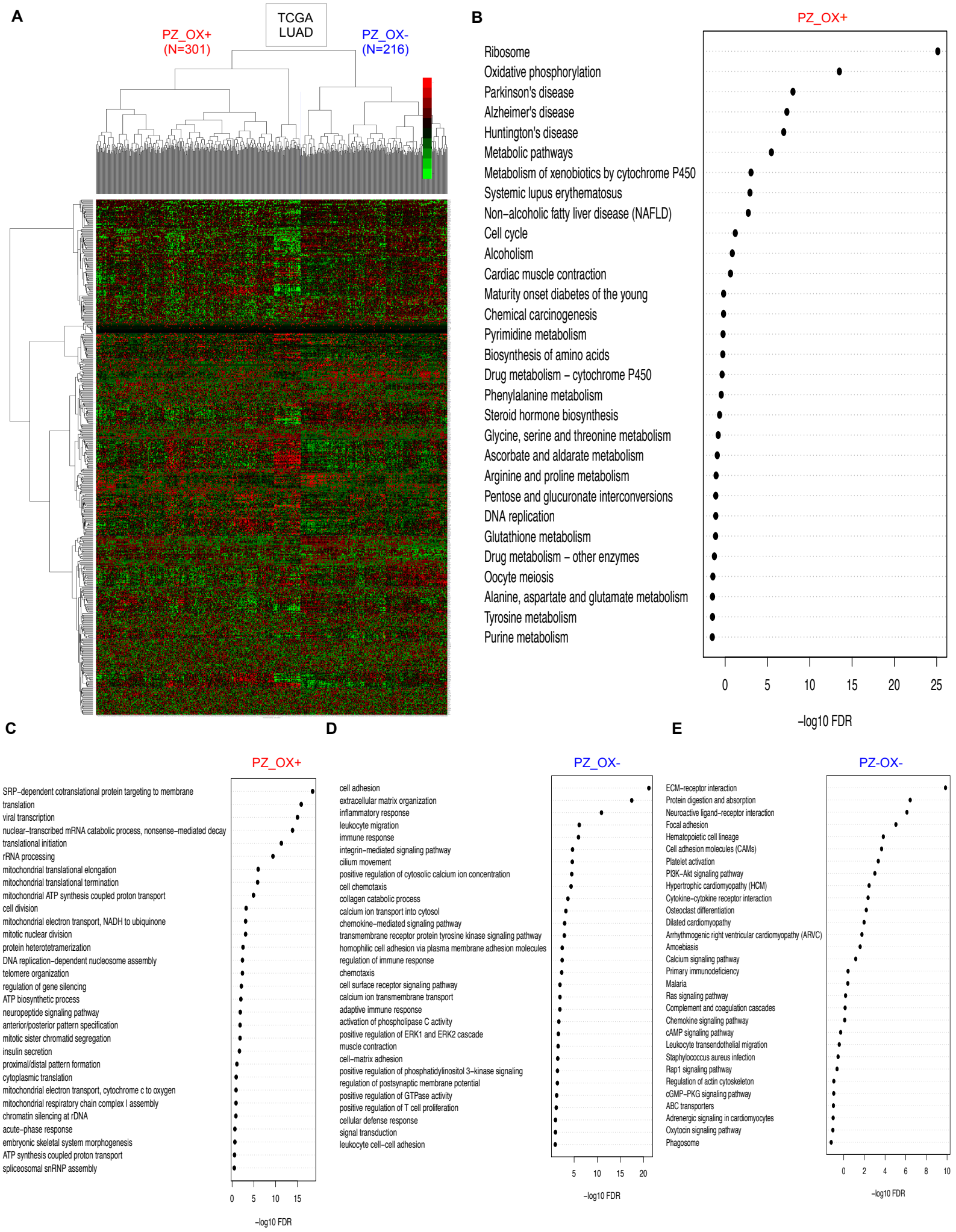

Figure S2: A) Hierarchical clustering of the TCGA-LUAD RNAseq data available from the Genomic Data Commons Portal (https://portal.gdc.cancer.gov/) using the full proteomic signature of oxidative tumors (OX^+PZ/OX^-PZ) determined from Figure S1A). **B)** Top 30 KEGG pathways and **C)** GO terms enriched in PZ_OX^+_LUAD tumors. **D)** Top 30 KEGG pathways and **E)** GO terms enriched in PZ_OX^-_LUAD tumors. For **B-E**, differential expression analysis was performed on TCGA RNA-Seq data using DESseq2 between OX^+ and OX^- LUAD tumors and genes were selected based on adjusted p-value (<0.05) and fold-change (>1.5). DEseq2 compares groups using a Wald test followed by a Bonferroni multiple test correction.

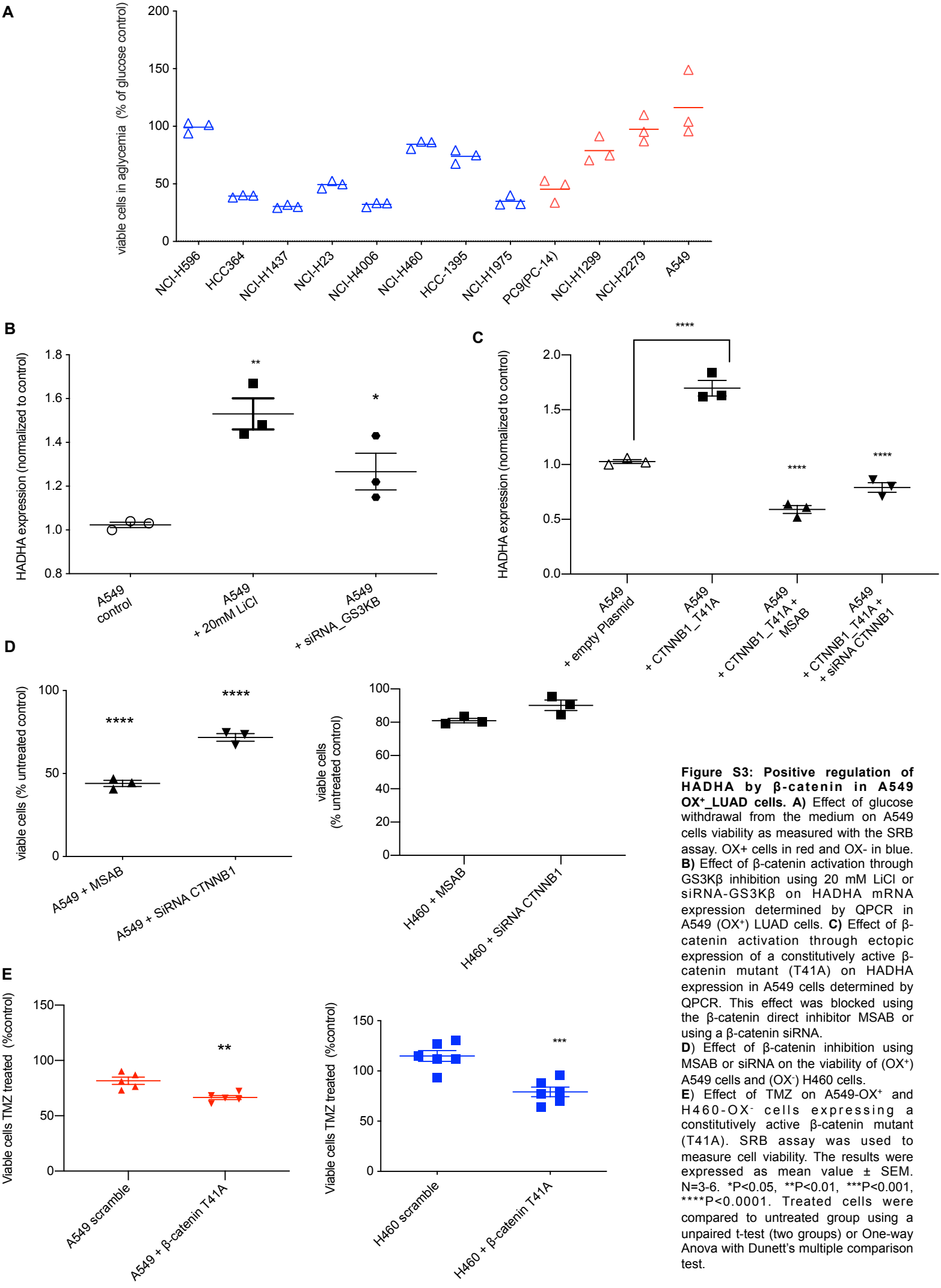

Figure S3: Positive regulation of HADHA by β-catenin in A549 OX⁺_LUAD cells. A) Effect of glucose withdrawal from the medium on A549 cells viability as measured with the SRB assay. OX+ cells in red and OX- in blue. **B)** Effect of β-catenin activation through GS3Kβ inhibition using 20 mM LiCl or siRNA-GS3Kβ on HADHA mRNA expression determined by QPCR in A549 (OX⁺) LUAD cells. **C)** Effect of β-catenin activation through ectopic expression of a constitutively active β-catenin mutant (T41A) on HADHA expression in A549 cells determined by QPCR. This effect was blocked using the β-catenin direct inhibitor MSAB or using a β-catenin siRNA.
D) Effect of β-catenin inhibition using MSAB or siRNA on the viability of (OX⁺) A549 cells and (OX⁻) H460 cells.
E) Effect of TMZ on A549-OX⁺ and H460-OX⁻ cells expressing a constitutively active β-catenin mutant (T41A). SRB assay was used to measure cell viability. The results were expressed as mean value ± SEM. N=3-6. *P<0.05, **P<0.01, ***P<0.001, ****P<0.0001. Treated cells were compared to untreated group using a unpaired t-test (two groups) or One-way Anova with Dunett's multiple comparison test.

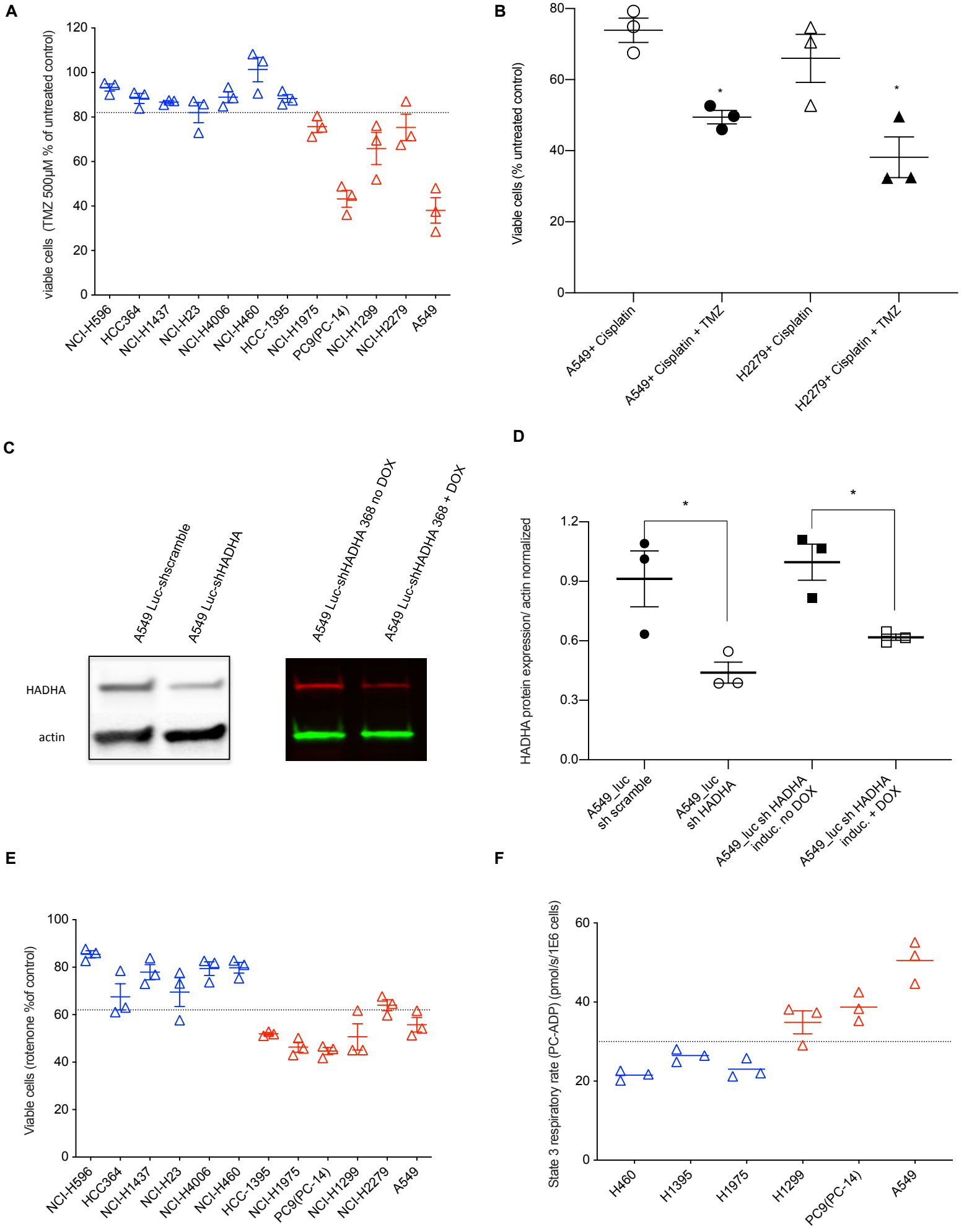

Figure S4: Pharmacological inhibition of HADHA in twelve NSCLC cancer cell lines. (A) The effect of HADHA inhibition by 500µM TMZ (24H) in OX+/HADHA+ (red) and OX-/HADHA- (blue) lung cancer cell lines was determined by measuring cell viability using the SRB assay. **(B)** Effect of TMZ 500µM in co-treatment with Cisplatin 30µM for 48H on cell viability. **C)** HADHA knock-down by shHADHA or by doxycyclin (DOX) inducible shHADHA verified by westernblot. **D)** Westernblot quantification of HADHA levels as normalized to actin level. **E)** Effect of rotenone treatment on OX+ (red) and OX- (blue) NSCLC cell lines. **F)** Rate of fatty-acid oxidation coupled to OXPHOS measured by high-resolution respirometry on permeabilized human lung cancer cells fueled with palmitoyl-carnitine (PC) and ADP. Cells with low capacity of palmitoyl-carnitine oxidation are shown in blue (OX-) and cells with high capacity (OX+) are shown in red. The dashed line shows the median value of palmitate fueled coupled respiration. The data are expressed as the mean value ± SEM . N=3. *P<0.05, **P<0.01, ***P<0.001, ****P<0.0001. The groups were comparing using a unpaired t-test (two groups) or One-way Anova with Dunett's multiple comparison test.

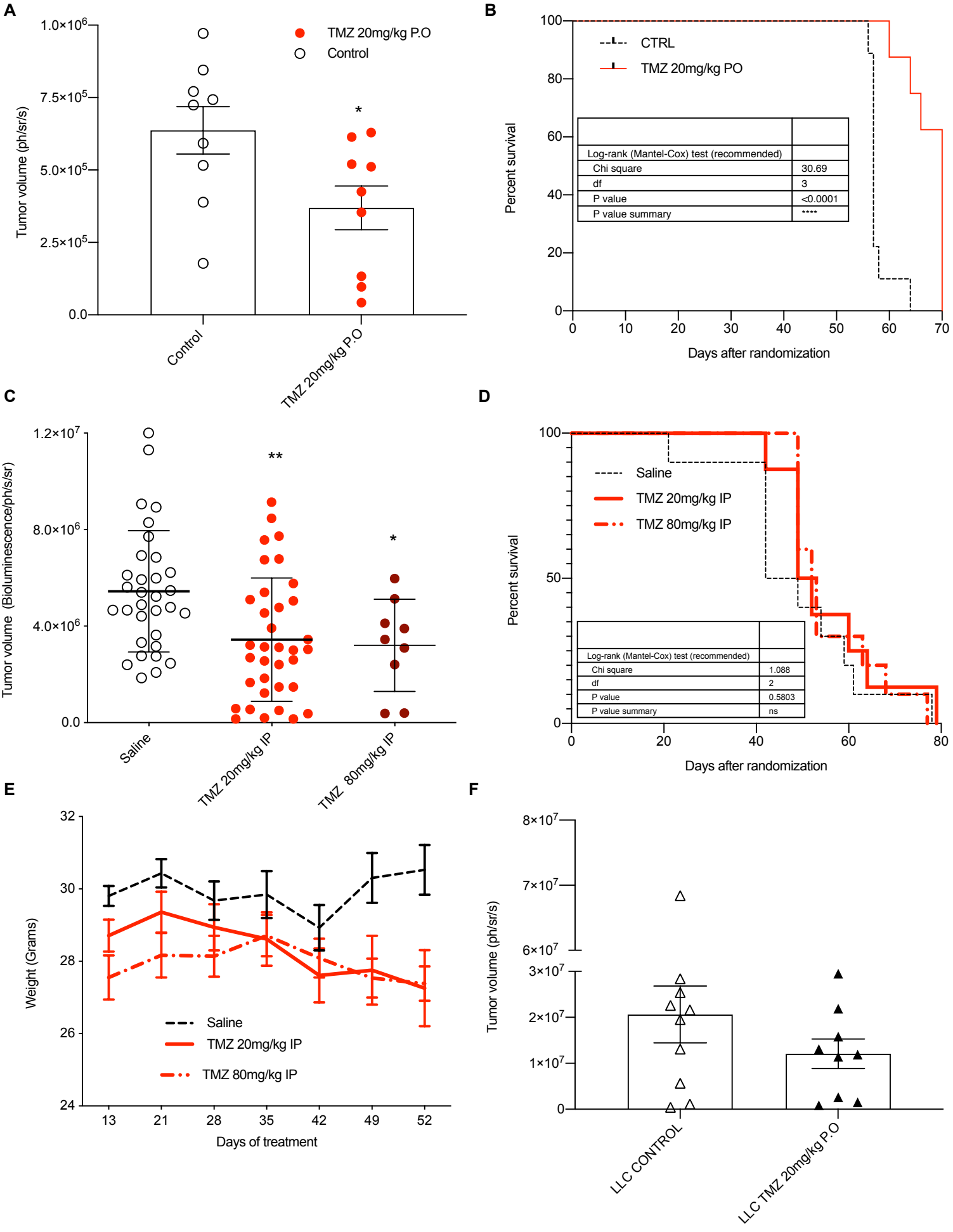

Figure S5. Anticancer effect of HADHA pharmacological inhibition using Trimetazidine administered by IP or PO on OX⁺_LUAD . A) Mice bearing orthotopic human lung adenocarcinomas obtained with OX⁺-LUAD_A549 cells were treated with TMZ 20mg/kg per oral (P.O). The volume of orthotopic A549luc-OX⁺_LUAD tumors was determined *in vivo* non-invasively using the luminescence signal. **B)** Survival curve obtained with TMZ 20mg/kg P.O treatment on A549 OX+_LUADs. **C)** Effect of intraperitoneal injection (IP) of TMZ on OX⁺_A549luc_LUAD volume. TMZ 20mg/kg or TMZ 80mg/kg was injected daily by IP. **D)** Survival curve obtained using TMZ 20mg/kg or 80mg/kg IP showing no significant effect. **E)** Body weight alteration in the animals treated with TMZ 20mg/kg or 80mg/kg by IP injection. **F)** Effect of TMZ 20mg/kg per oral (PO) administration in a immunocompetent mouse LUAD model obtained with murine LLC lung cancer cells in syngenic animals. Values represent mean ± SEM; N=10-30 for each group. *P<0.05, **P<0.01, ***P<0.001. Treated animals were compared to untreated group using One-way Anova with Dunett's multiple comparison test. Survival curves were compared using Log-rank (Mantel-Cox) test.

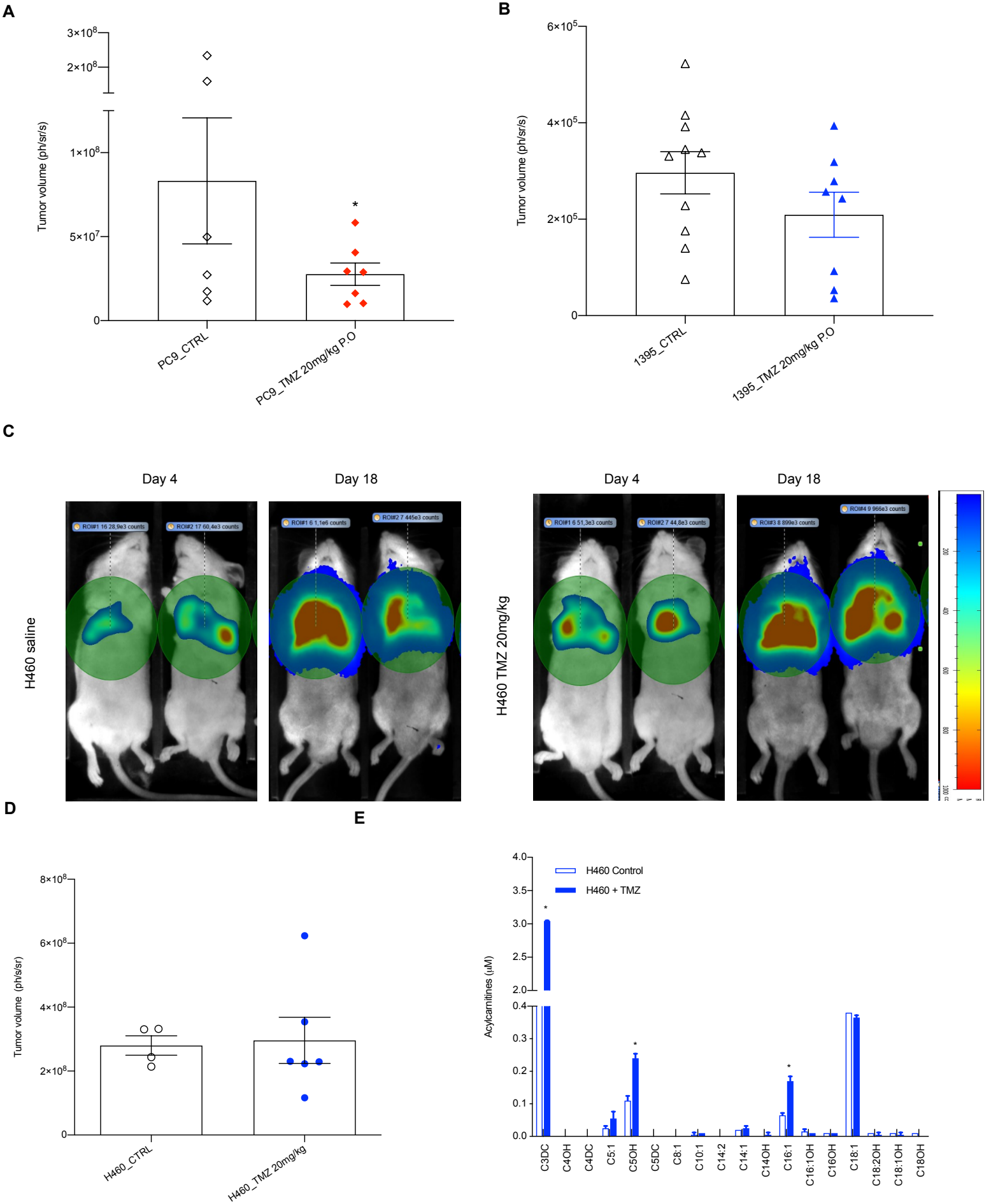

Figure S6: TMZ inhibits specifically OX+ lung tumor growth. Lung tumor growth was determined by the bioluminescence of human cancer cells injected orthotopically in the lung of NSG mice, after 18 days of growth**. A)** Results for the HADHA+/OX+ PC9 NSCLC cells and **B)** for theHADHA-/ OX- 1395 cells. The animals were treated with vehicle or TMZ (20 mg/kg) daily P.O for 18 d (*n* = 10 mice per group). **C and D**) Relative volume of HADHA-/OX- H460 orthotopic tumors determined in mice treated with vehicle (saline) or TMZ (20 mg/kg) daily for 18 d (*n* = 10 mice per group). **E)** Lipidomic analysis (mass spectromerty) of fatty-acids accumulating in H460 cells (OX-) cells treated with 500µM TMZ during 48 hours. Values represent mean ± SEM; N=4-6; N=10 *in vivo* experiments for each group. *P<0.05, **P<0.01, ***P<0.001. Treated animals were compared to untreated group using a unpaired t-test.

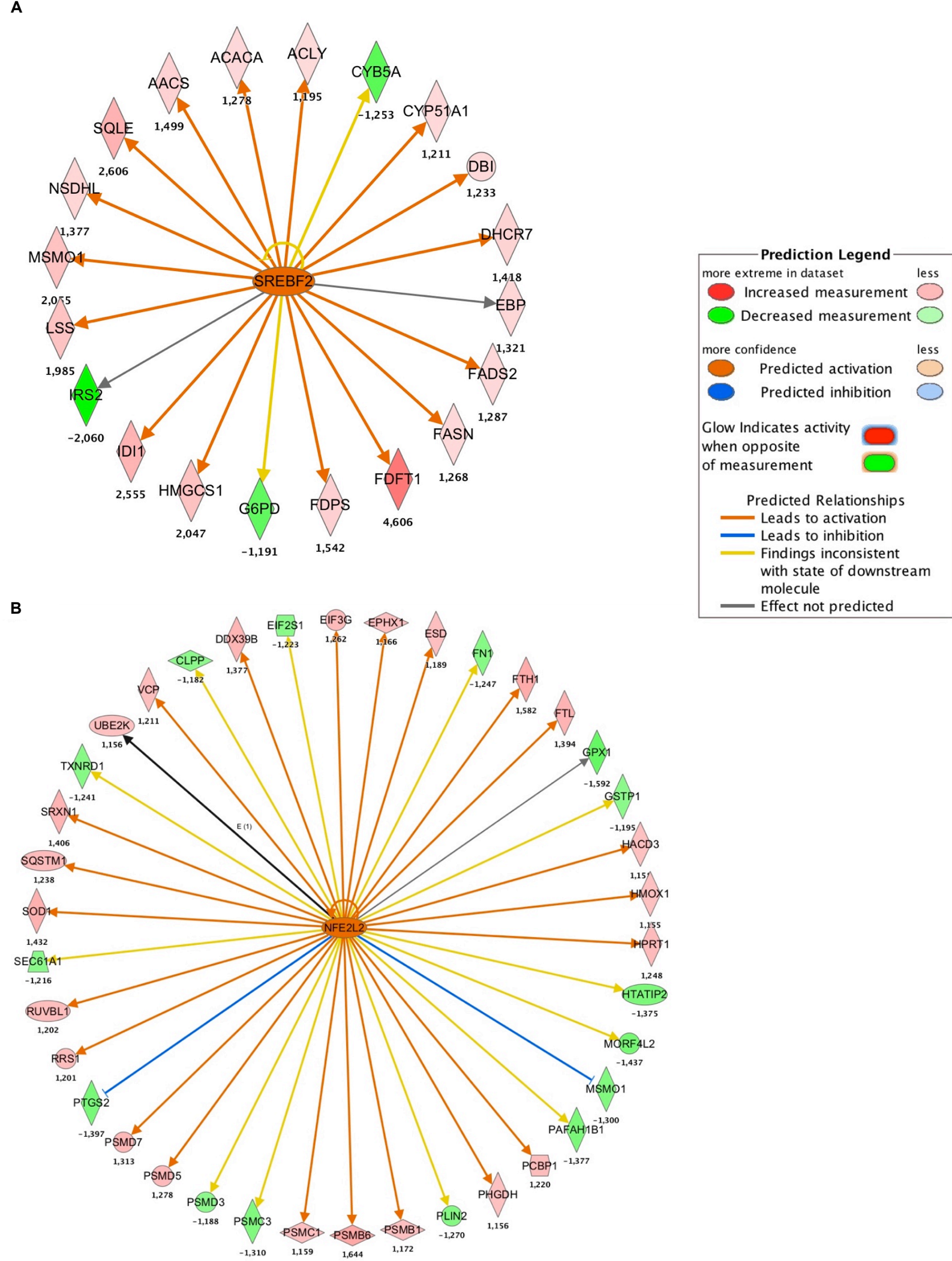

Figure S7: Predicted transcription factors activated following HADHA inhibition using TMZ or shHADHA in human lung adenocarcinoma A549 cells. (A) SREBF2. **(B)** NRF2. The prediction analysis was performed using IPA (Qiagen). The proteins altered by HADHA inhibition ($p<0.05$) were analyzed using the 'upstream analysis' module of IPA.

Full unedited gels (Amoedo N.D et al.)

Figure 3 (uncropped)

Gel #1 HADHA NSCLC cell lines

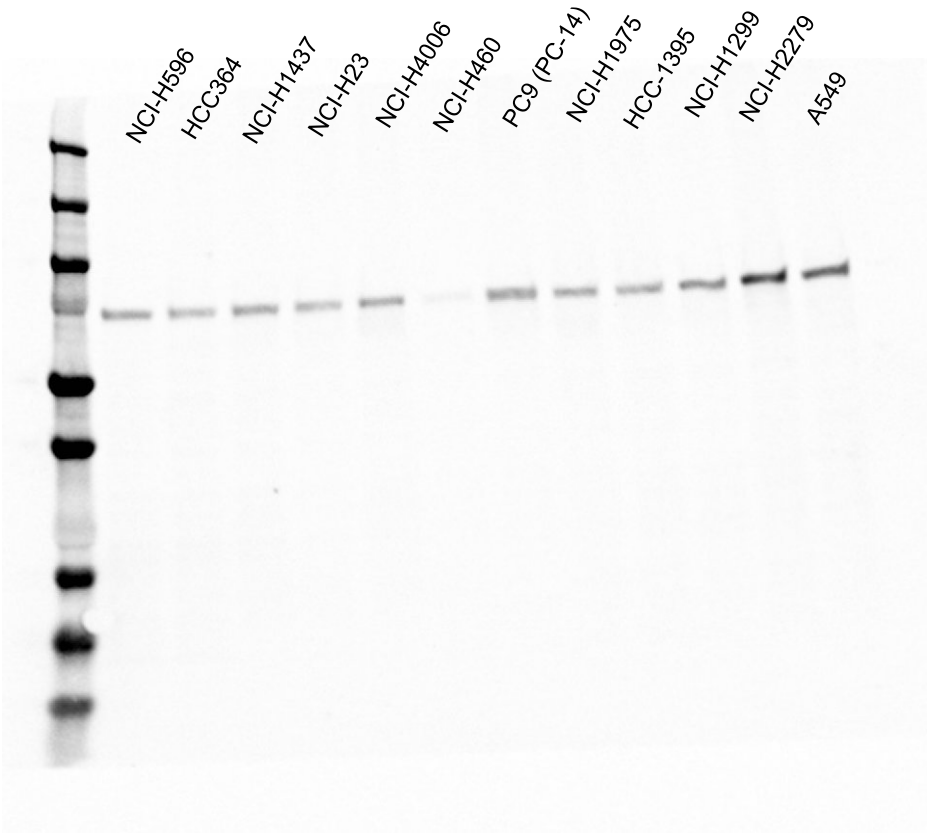

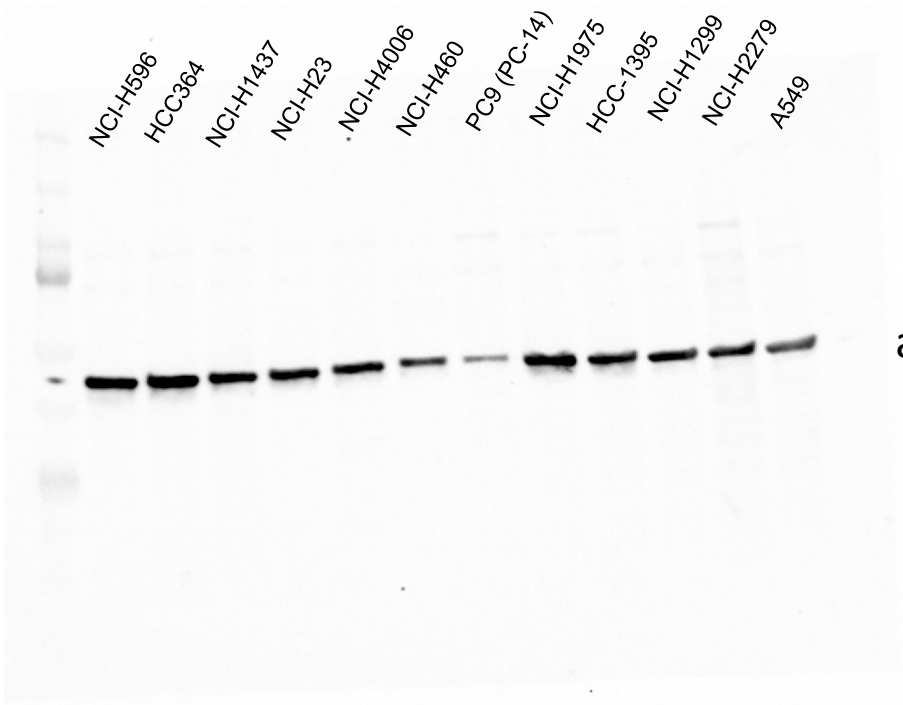

Figure 3 (uncropped)

Gel #2 HADHA NSCLC cell lines

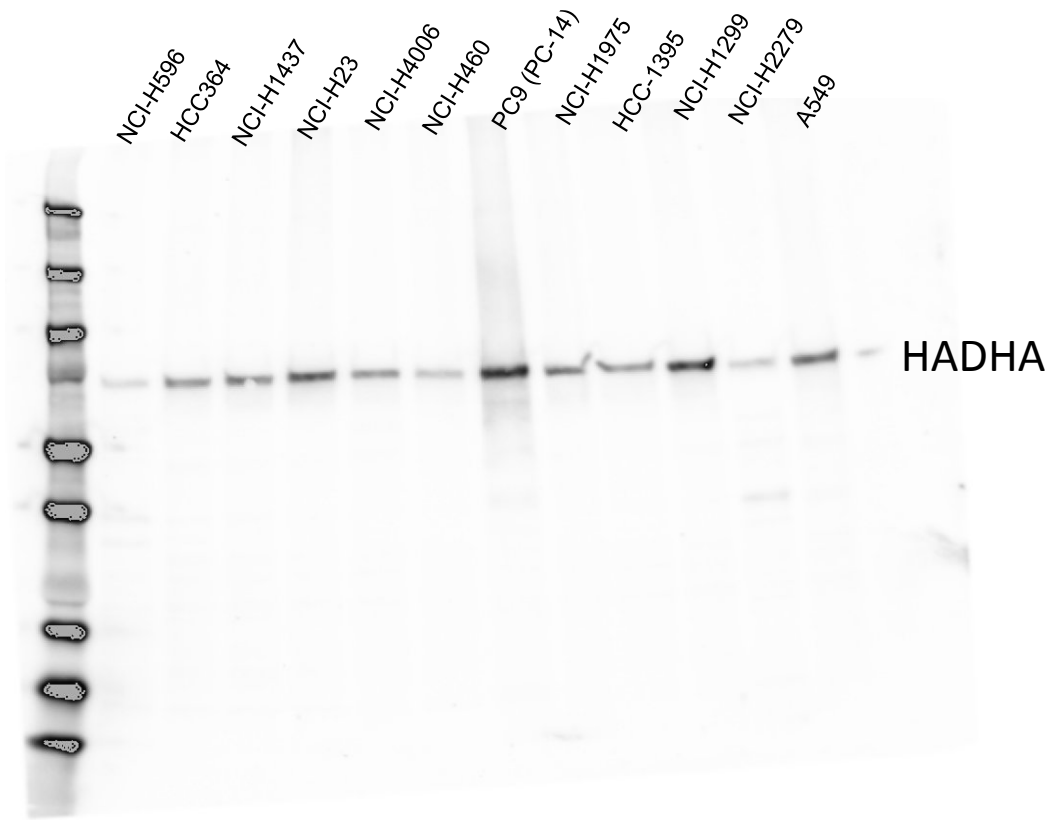

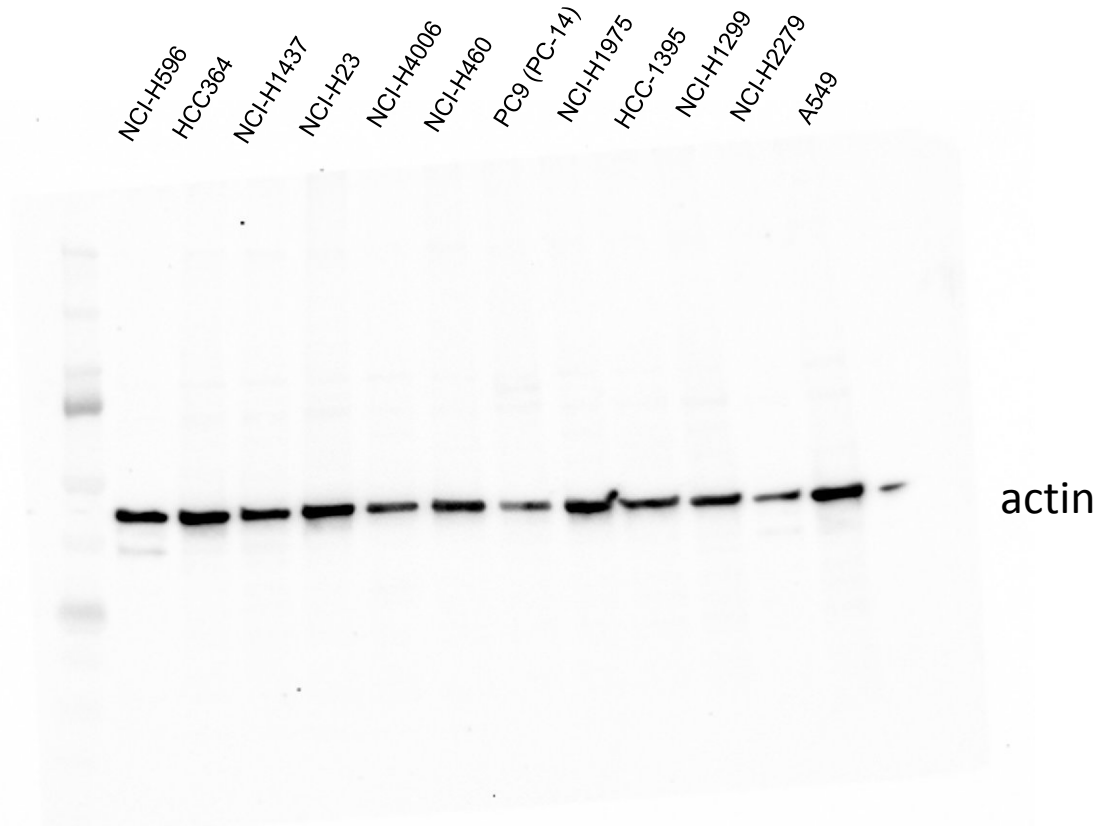

Figure 3 (uncropped)

Gel #3 HADHA NSCLC cell lines

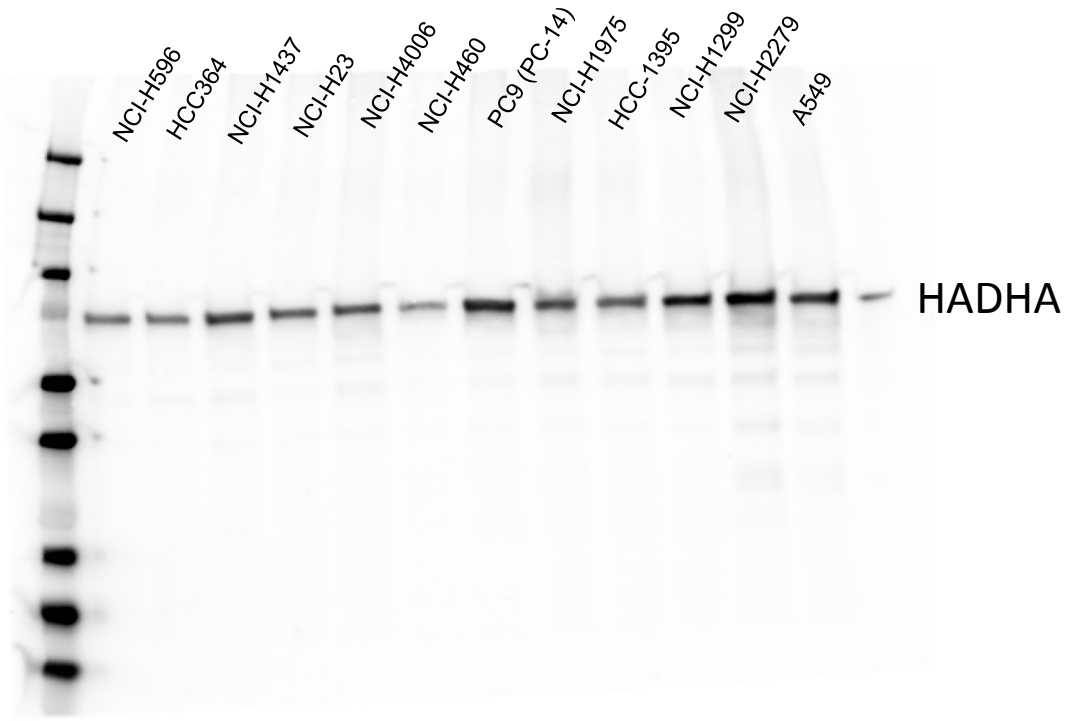

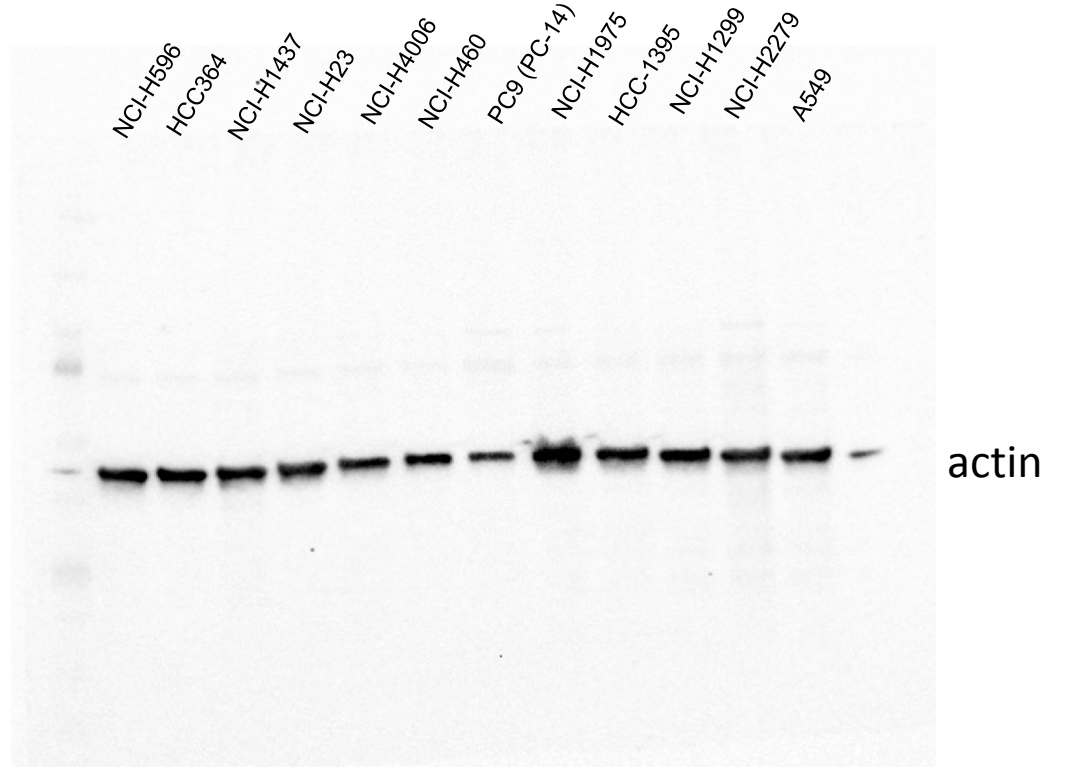

Figure S4 (uncropped)

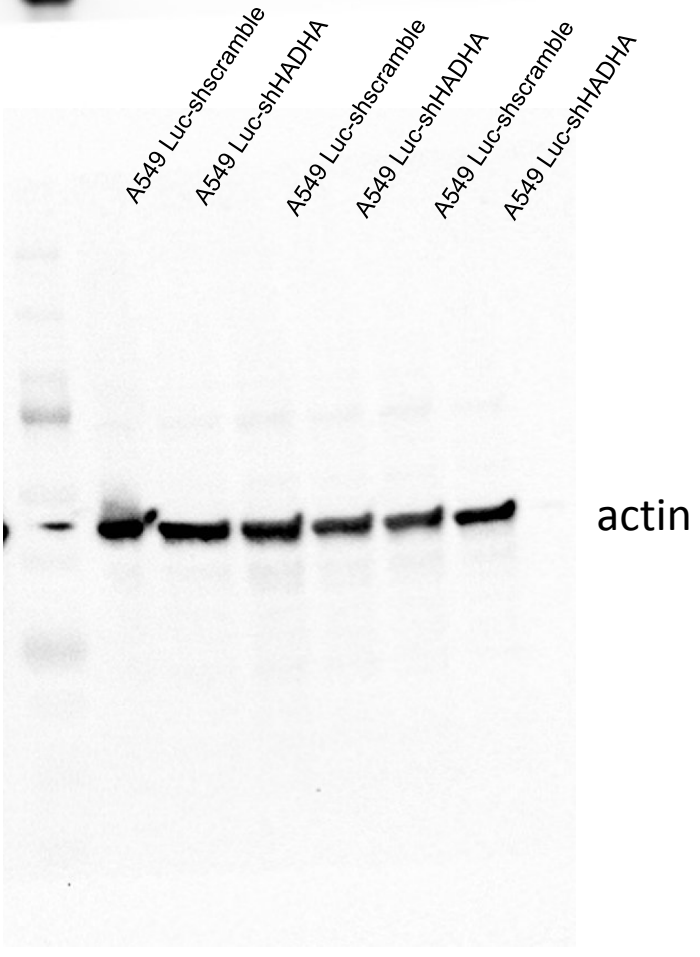

Figure 6 (uncropped)

STAIN FREE

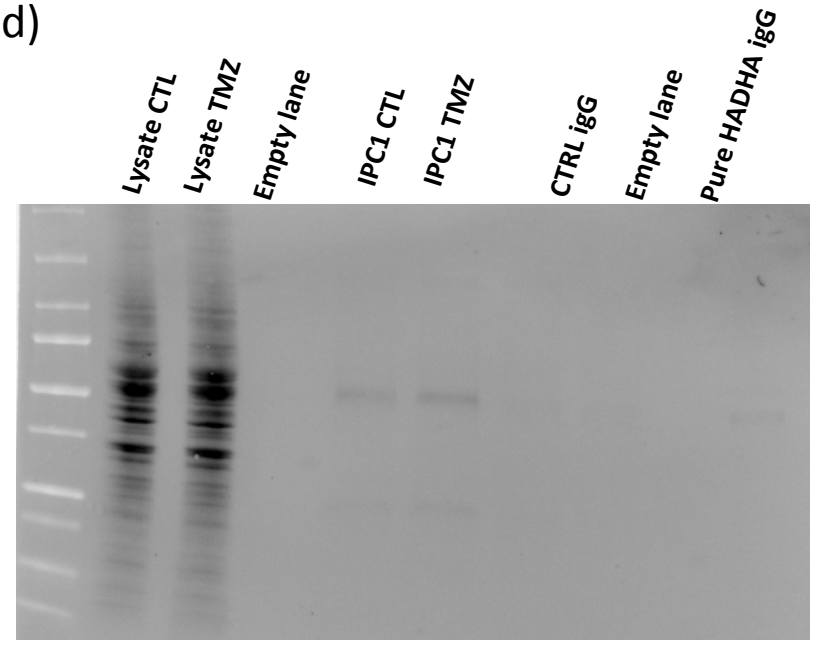

Western blot

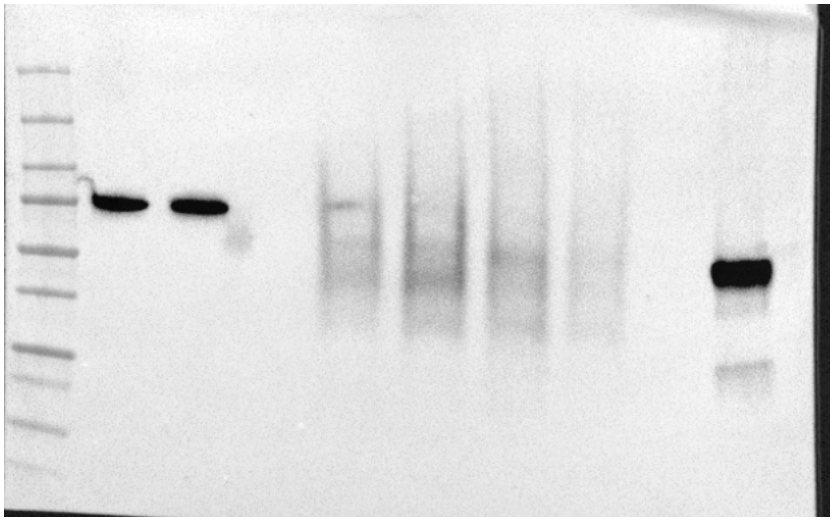

Ref. Ac HADHA ab203114 (MW 75kDa)